Sensors & Actuators: B. Chemical 390 (2023) 133932

Contents lists available at ScienceDirect

Sensors and Actuators: B. Chemical

journal homepage: www.elsevier.com/locate/snb

Anisotropic aerogel induced gelatin hydrogel actuator with favourable mechanical properties and multiple solvent responsiveness

Zhongwen Kuang [a,1], Weizhong Xu [a,b,1], Jiaxin Li [a], Zhuanzhuan Fan [a], Ruofei Wang [a], Shanpeng Ji [a], Chengnan Qian [a], Lin Cheng [a], Huaping Wu [c], Aiping Liu [a,*]

[a] Key Laboratory of Optical Field Manipulation of Zhejiang Province, Zhejiang Sci-Tech University, PR China
[b] Institute of Biomedical & Health Engineering, Shenzhen Institute of Advanced Technology (SIAT), Chinese Academy of Science (CAS), Shenzhen 518035, PR China
[c] Key Laboratory of Special Purpose Equipment and Advanced Processing Technology, Ministry of Education and Zhejiang Province, College of Mechanical Engineering, Zhejiang University of Technology, Hangzhou 310023, PR China

ARTICLE INFO

Keywords:
Directional freezing
Anisotropic aerogel
Gelatin hydrogel actuator
Multiple solvent responsiveness
Intelligent valve

ABSTRACT

As an important part of biomimetic/intelligent new materials, the hydrogel actuator can sense changes in the external environment and convert external energy into mechanical energy, therefore attracting extensive attention in many fields. However, the relative weak mechanical properties, small driving force and single responsiveness to external stimuli of hydrogel-based actuators are still the main factor restricting their practical application and future development. In this paper, a heterogeneous hydrogel-based actuator with favourable mechanical properties and multiple solvent responsiveness is constructed via the synergistic action of anisotropic chitosan aerogel as the skeleton and solvent-sensitive gelatin hydrogel as muscle in the actuator framework. The addition of aerogel skeleton and the salting out of gelatin favor the actuator favourable mechanical behavior with maximum tensile stress and compressive stress up to MPa level. Furthermore, the heterogeneous aerogel/hydrogel composite structure greatly improves the driving capability of actuator, presenting multiple solvent responsiveness with the maximum driving amplitude up to 730° in the ion solution. The well-designed actuators can be exploried as intelligen microfluidic valves that recognize and pass specific solutions at different flow rates. This aerogel/hydrogel composite actuator has broad application prospects in microfluidic systems, smart valves, artificial muscles and intelligent human-machine interaction.

1. Introduction

Hydrogel is a kind of three-dimensional crosslinked polymer material with high water content, which is widely used in coatings [1], adhesives [2], implantable electronics [3], energy storage devices [4], tissue engineering [5], drug delivery [6], and artificial muscles [7]. The responsive hydrogel can be triggered by pressure [8,9], temperature [10,11], light [12–14], pH [15,16], ions [17,18], solvents [19,20], electric [21,22] and magnetic fields [23] and other specific external stimulus and present three-dimensional controllable and programmable shape transformation, therefore attracting many research interests as environment-responsive actuators [24–26]. However, there are still some problems in the research and practical application of hydrogel actuators. Firstly, homogeneous hydrogels usually achieve macro expansion/contraction under the uniform external stimulus. In order to realize specific deformation, various anisotropic structures need to be designed and fabricated for the hydrogel actuators, including bilayer structures [10,15,16], gradient structures [14,27], graphic structures [21], directional structures [20,28], and other anisotropic structures [11,18,23]. Secondly, the high water content and weak crosslinking action of hydrogels make them soft and fragile in practical applications. Although various advances have been reported in toughening hydrogels by forming dual networks [29], adding nanofillers [30] and proceeding mechanical training [31], there is still a significant difference in the mechanical property when compared to anhydric polymers [32]. The driving behaviors of these toughening hydrogels have also been not given enough attention. Therefore, how to improve the mechanical properties and deformation capacity of responsive hydrogel actuators is an important concern in the wide application of hydrogel actuators.

Consider the skeletal and muscular system of the human body

* Corresponding author.
E-mail address: liuaiping1979@gmail.com (A. Liu).
[1] Zhongwen Kuang and Weizhong Xu contributed equally.

https://doi.org/10.1016/j.snb.2023.133932
Received 13 January 2023; Received in revised form 30 April 2023; Accepted 3 May 2023
Available online 6 May 2023

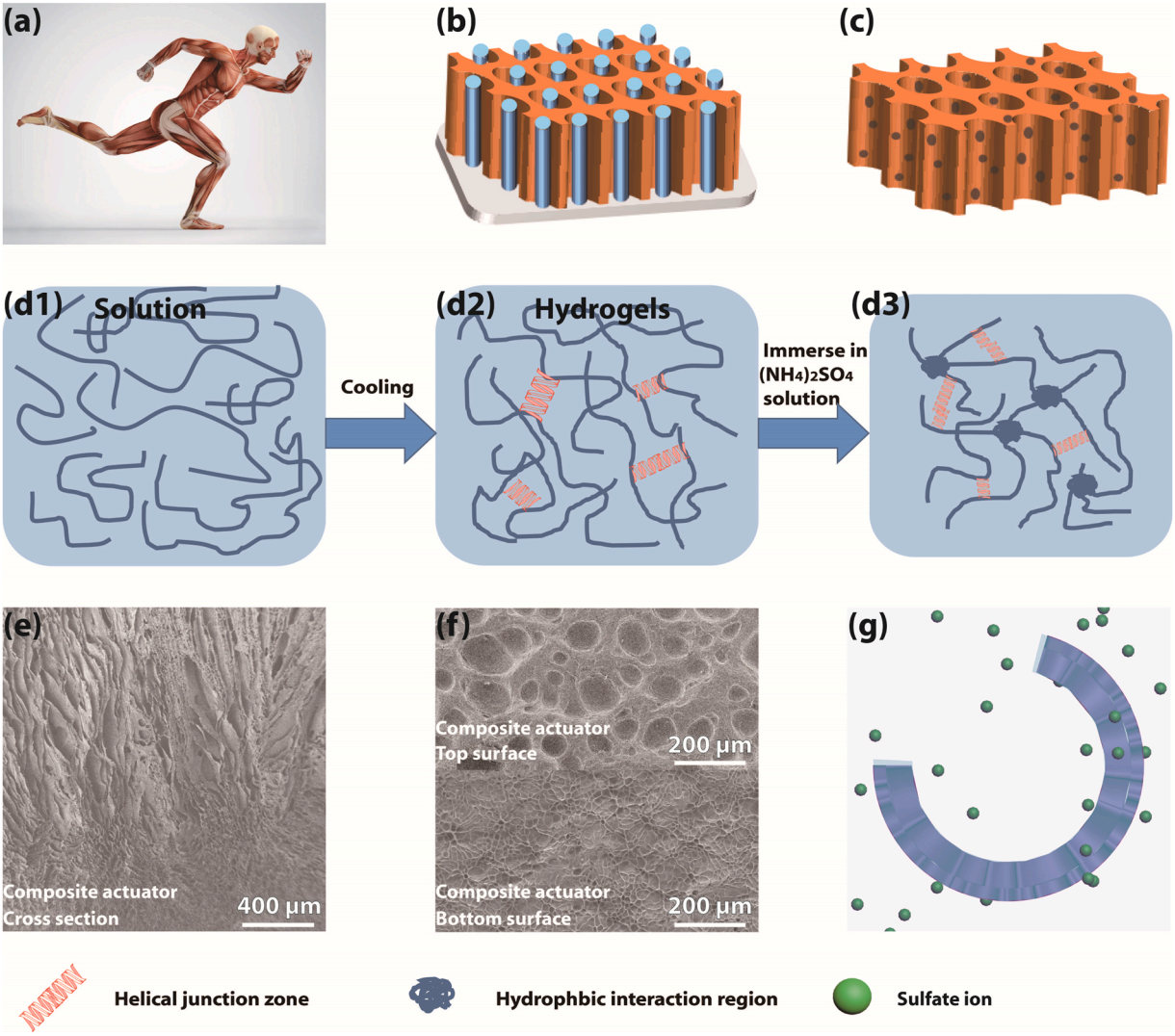

Fig. 1. Preparation and driving process of chitosan aerogel/gelatin hydrogel composite actuator. (a) Schematic diagram of the skeletal and muscular system of human body, (b) schematic diagrams of aerogel formation by the ice template method and (c) the obtained chitosan aerogel after freeze drying. (d) Schematic diagram of shrinkage principle of gelatin hydrogel: (d1) gelatin solution, (d2) gelation process, (d3) salting out effect of gelatin hydrogel in $(NH_4)_2SO_4$ solution, (e-f) scanning electron microscope (SEM) pictures of chitosan aerogel/gelatin hydrogel composite: (e) cross section diagram of composite, (f) top and bottom surfaces of composite, (i) schematic diagram of driving process of composite actuator in the ionic solution.

(Fig. 1a). The skeleton supports the body, provides the sites for muscle attachment, and assists the muscles to perform the action and so on. The muscles we usually talk about are skeletal muscles because of their attachment to bones by tendons. Skeletal muscles can produce total or partial contraction in response to a stimulus, move bones and joints and enable us to perform a wide variety of postures and movements. Inspired by the anatomy of the human body, we propose a fascinating aerogel/hydrogel composite structure as smart actuator, namely an anisotropic chitosan aerogel as the skeleton and gelatin hydrogel which is filled into the aerogel as the responsive muscle. The simple and environmental-friendly ice template method is used to prepare directional porous chitosan aerogel materials with stable structure (Fig. 1b-c, Fig. S1). When the temperature is higher than the upper critical dissolving temperature of gelatine (40 ℃), it presents an random coil structure in the solution (Fig. 1d1) [33]. At low temperature, the gel molecules are connected by hydrogen bonds to form a stable helical region, thus forming hydrogel (Fig. 1d2). After the pre-formed gelatin hydrogel is soaked in a $(NH_4)_2SO_4$ solution, the solubility of gelatin is reduced due to salting out effect, and the gelatine molecular chain gathers and binds, resulting in water discharge and volume shrinkage (Fig. 1d3) [33]. The good combination of anisotropic aerogel and responsive hydrogel (Fig. 1e) not only successfully improves the mechanical properties of the actuator with the maximum tensile stress up to 1.9 MPa and the maximum compressive stress up to 3.5 MPa, but also induces the nonhomogeneous structure of composite (Fig. 1f), making it possible to bend in a variety of ionic solutions (Fig. 1g) and organic solvents (the maximum driving amplitude up to 730°, details in bending angle measurement shown in Fig. S2), and restore to the initial state after being put into deionized water. The well-designed composite actuator can be developed as an intelligent microfluidic valve that can identify the specific fluid flow and control the flow rates for different solutions. The proposed strategy provides a simple and green method for structuring responsive hydrogels, foreshadowing application prospects in intelligent actuators, soft robots, microfluidics systems and intelligent human-machine interfaces.

2. Materials and methods

2.1. Materials

Gelatin (photographic grade, adhesive strength ~ 260 g Bloom),

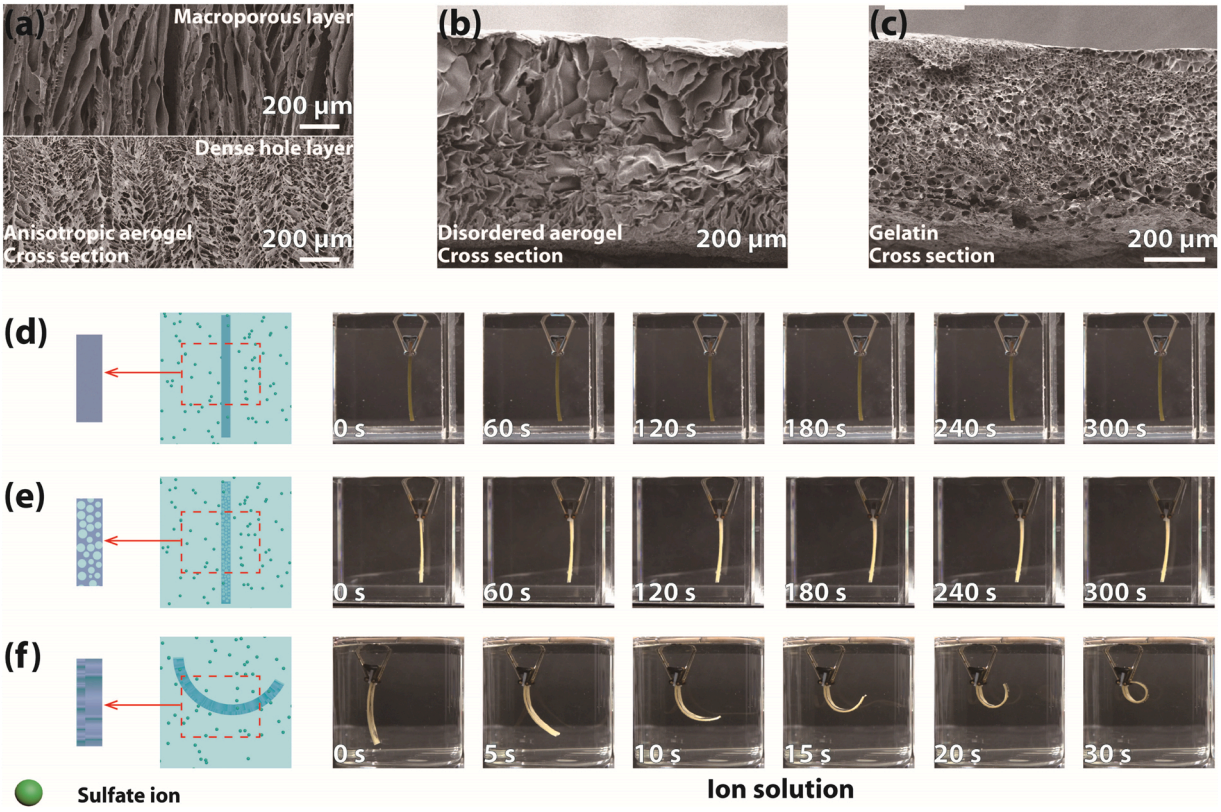

Fig. 2. Morphology and driving mechanism of chitosan aerogel/gelatin hydrogel composite actuator. Cross section SEM images of (a) macroporous layer and dense hole layer of composite with ordered chitosan aerogel, (b) disordered chitosan aerogel and (c) pure gelatin. (d)-(f) Schematic diagrams and optical photos of bending deformation of (d) pure gelatin, (e) composite actuator with disordered chitosan aerogel and (f) composite actuator with ordered chitosan aerogel in the $(NH_4)_2SO_4$ solution.

chitosan (CS, low viscosity: < 200 Mpa s), glacial acetic acid (GAA), glutaraldehyde (GA), sodium hydroxide (NaOH), ethanol, ammonium sulfate ($(NH_4)_2SO_4$), sodium carbonate (Na_2CO_3), sodium thiosulfate ($Na_2S_2O_3$), sodium dihydrogen phosphate (NaH_2PO_4), sodium acetate (CH_3COONa), sodium chloride (NaCl), dimethyl sulphoxide (DMSO), isopropano (IPA), glycol (EG), acetone (TATP), ethyl alcohol (ETOH) were all purchased from Shanghai Maclin Biochemical Co., LTD. (China). Deionized water (18.2 MΩ, 25 ℃) from water purification system (UPT-I-10, China) was used in the whole experiment. All reagents were of analytical grade and no purification was carried out.

2.2. Preparation of chitosan aerogel by ice template method

First, a 2 wt% chitosan solution with glacial acetic acid was injected into a mold consisting of copper sheets, silica gel sheets and glass slides (40 mm × 10 mm×1 mm in length×width×height). Then the mold was placed on the pre-cooling refrigeration device with the copper sheet close to the cold source, so that the temperature formed directional conduction from the copper sheet upward, and the chitosan solution turned into anisotropic flake ice (Fig. S1). After the samples were completely frozen, they were moulded, freeze-dried, and immersed in 0.4% NaOH ethanol solution for 30 min to remove glacial acetic acid. Finally, the sample was frozen again and then freeze-dried, so that the anisotropic chitosan aerogel skeleton with aligned structure was obtained. Different directional freezing temperatures including − 30 ℃, − 60 ℃ and − 90 ℃ were set to prepare chitosan aerogel skeleton. In a similar way, the chitosan aerogel with disordered structure was also prepared by a random freezing process.

2.3. Preparation of aerogel/hydrogel composite actuator

A 10 wt% gelatin solution was added to the chitosan aerogel skeleton with ordered structure and placed in an environment of 4 ℃. Then the sample was immersed in 1% glutaraldehyde solution (physical crosslinking agent) at room temperature to crosslink for 8 h, obtaining chitosan aerogel/gelatin hydrogel composite (40 mm × 10 mm×1 mm in length×width×height). Analogously, an aerogel/hydrogel composite with disordered chitosan aerogel as the skeleton was also prepared as a control.

2.4. Characterization

Morphology and microstructure of chitosan aerogel and gelatin hydrogel were observed by scanning electron microscope (SEM, S-4800, Hitachi) under 5 kV acceleration voltage. Before test, the samples were freeze-dried in a freeze dryer (FD-1A-80, China) at − 80 ℃. The melting of gelatin hydrogel was analyzed on a differential scanning calorimeter (DSC, TA DSC Q200, USA) in the temperature range from 20 ℃ to 250 ℃ at a scanning rate of 5 ℃min^{-1} under nitrogen atmosphere. The crystalline structure of lyophilized gelatin was characterized by X-ray diffractometer (XRD, D8 discover, Purrucker) in the scanning speed of 5 ℃min^{-1}. Fourier transform infrared (FTIR) spectroscopy was recorded on an infrared spectrometer (Thermo scientc, NicoletiS50 series) with a wavenumber range of 500–4000 cm^{-1}. To explore the mechanical properties, tensile and compression experiments were carried out on a mechanical testing machine (Legendary 2366 INSTRON) with the tensile speed of 50 mm/min and compression speed of 10 mm/min. The compressed sample was made into 10 mm × 10 mm× 10 mm cube, and the stretched sample was made into 40 mm × 10 mm× 1 mm cuboid. After calculating and analyzing the relationship between force and

deformation, the stress-strain curve and modulus diagram were obtained. The water content of gelatin hydrogel (F_{water}) was measured by calculating the percentage of mass change of gelatin before and after freeze-drying with liquid nitrogen, namely $F_{water}= [(m_w\text{-}m_d)/m_w]\times 100\%$. Here m_w and m_d were the weight of gelatin before and after freeze drying.

To study the bending behavior of the composite actuator, one end of the hydrogel was held in place with a clamp and the other end was suspended freely in the air. Then the sample was put into the $(NH_4)_2SO_4$ solutions with different concentrations (1 mol/L, 2 mol/L, and 3 mol/L) to drive, and then put it back into deionized water to recover. The driving behaviors of composite actuator in other different kinds of ionic solutions (sodium carbonate, sodium thiosulfate, bisdicarbonate sodium, sodium acetate and sodium chloride) and different organic solutions (dimethyl sulphoxide, isopropano, glycol, acetone and ethyl alcohol) were also evaluated. The entire deformation process was filmed with a digital camera and screenshots were taken at various time pointes. The bending angle of the composite actuator in the screenshot (Fig. S2) was measured by Image J software, and the relationship between bending angle and time was investigated.

3. Results and discussion

3.1. Effect of aerogel microstructure on driving behavior of composite actuator

Ice template method is widely used to prepare oriented porous materials via ice crystals directional freezing and growing [34–36]. Through controlling temperature gradient of frozen elements (chitosan solution), the solution first crystallizes and nucleates on the freezing surface, and then grows along the temperature gradient to form ice crystals with directional structure, obtaining a directional gradient structure of chitosan aerogel skeleton. As shown in Fig. 2a, the chitosan aerogel skeleton presents two different structures, namely dense holes layer on the lower side (nucleate formation layer) and directional macropore layer on the upper side (crystal growth layer). Chitosan aerogel is insoluble in water after the removal of acetic acid, and has a stable structure that is unbreakable [36]. By comparison, the chitosan aerogel prepared under random frozening process displays a disordered porous structure with the chitosan lamella mussily piled up (Fig. 2b) due to the lack of temperature gradient. Gelatin is a kind of macromolecule hydrophilic colloid, which has a random coil structure when the temperature higher than 40 ℃, and forms a stable gel due to the connection of hydrogen bonds between gelatin molecules when the temperature lower than 40 ℃ (Fig. 1d2) [33]. As a protein, gelatin has a characteristic of salting-out effect, namely the gelatine hydrogel will shrink due to salting out in ionic solution, and expand and recover again in deionized solution [33]. This response to salt solution of gelatin makes it a potential as an ionic-responsive actuator. Fig. 2c shows the structure of gelatine hydrogel with uniformly dispersed dense holes, and the aperture size is distributed in 10–50 μm range. When the gelatin solution was added to the chitosan aerogel skeleton with directional structure and gelatinized in a low temperature environment to form composite, the anisotropy gradient structure can be obviously observed on the cross section (Fig. 1g), and the aperture of the top surface is much larger than that of the bottom surface (Fig. 1h). The close conbination between chitosan aerogel and gelatin hydrogel (gelatin is filled into the aerogel skeleton) is vital when the composite is used as a responsive actuator. For pure gelatin hydrogel with homogeneous structure, only macro expansion/contraction without nonplanar bending deformation can be observed under the uniform external stimulus (Fig. 2d). When the gelatin hydrogel combinates with the disordered porous chitosan aerogel, the isotropous skeleton and muscle system only presents a faint response to the $(NH_4)_2SO_4$ solution (Fig. 2e). By contrast, the chitosan aerogel with directional ordered structure can favor the composite system more structural differences, inducing an obvious bending deformation towards directional macropore end due to the dominant proportion of gelatin and volume shrinkage after sailing out of gelatin in directional macropore layer (Fig. 2f).

Additionally, the directional freezing temperature also affects the microstructure of aerogel skeleton and the driving performances of composite actuator. When the composite actuator is driven, the force generated by the contraction of gelatin in the directional large hole layer is larger than that of dense hole layer. We define the difference between the two forces with gravity deduction as the driving force of the composite actuator, so the larger the proportion of the directional large hole layer, the greater the driving force of the composite actuator. We set three directional freezing temperatures of − 30 ℃, − 60 ℃ and − 90 ℃ to prepare aerogel skeleton with 3 mm thickness, respectively. With the decrease of directional freezing temperature, the thicknesses of dense hole layers at the bottom are about 1020 μm (−30 ℃), 505 μm (−60 ℃) and 115 μm (−90 ℃), respectively, and the thickness ratios of large hole layer to dense hole layer are about 2:1, 5:1 and 29:1, respectively (Fig. S3a-c). This means that the time for crystallization and nucleation is shorter with the decrease of freezing temperature, and the dense hole layer related to crystallization and nucleation is thinner. Therefore, the greater thickness difference between the two layers for the composite actuator prepared at − 90 ℃ will present better driving performance. The scanning electron microscope (SEM) images of chitosan aerogel prepared at different directional freezing temperatures also demonstrate that the pore sizes of bottom surfaces for all aerogel skeleton are almost the same, while the pore sizes of top surfaces reduce with decreasing of freezing temperature (Fig. S3d-i). When the composite actuators (thickness of 1 mm) were immersed into a 3 mol/L $(NH_4)_2SO_4$ solution, the driving speed, maximum bending angle and recovery speed of the composite actuator in deionized water reaches the maximum for − 90 ℃ prepared sample (Fig. S4, Movie S1). The experimental phenomenon verifies that the structure of aerogel skeleton determines the driving capability and driving performance of the composite actuator. The lower the temperature of the aerogel skeleton made by ice template method, the better the driving performance of the composite driver.

Supplementary material related to this article can be found online at doi:10.1016/j.snb.2023.133932.

3.2. Effect of gelatin salting-out on driving behavior and mechanical property of composite actuator

It is well known that protein will condense and precipitate out of the solution when inorganic salts are added into the protein solution. This process is reversible, namely protein can be dissolved again after the system diluted with water. As a fat-free high protein, gelatin usually goes through the salting-out and dissolve process (Fig. S5). This is because the solubility of gelatin in water depends on the degree of hydration of hydrophilic group of the gelatin molecule with water and the charge of the gelatin molecule. After adding the $(NH_4)_2SO_4$ solution into gelatin solution, the affinity between anion and water molecules is greater than that between gelatin and water molecules, which increases the surface tension of the cavity around the gelatin molecular chain, resulting in the weakening or even disappearance of the hydration layer around the gelatin molecule (Fig. S6a) [37,38]. At the same time, the charge on the protein surface is largely neutralized due to the change of ion strength around gelation molecules, which damages the stability of the hydrogen bond between the polymer and its hydrated water molecules, leading to the decrease of the solubility of gelatin and the aggregation/precipitation of gelatin molecules (Fig. S6b) [37,38]. When gelatine hydrogel is formed in low temperature environment and then is immersed in $(NH_4)_2SO_4$ solution, gelatine hydrogel will not produce precipitation, but present volume shrinkage and water discharge due to the stable formation of gelatine molecule network through helical junctions (Fig. 1d3) at low temperatures [33]. This is well supported by the FTIR data. When the preformed gelatin hydrogel was immersed in $(NH_4)_2SO_4$ solutions of different concentrations (1 mol/L, 2 mol/L and

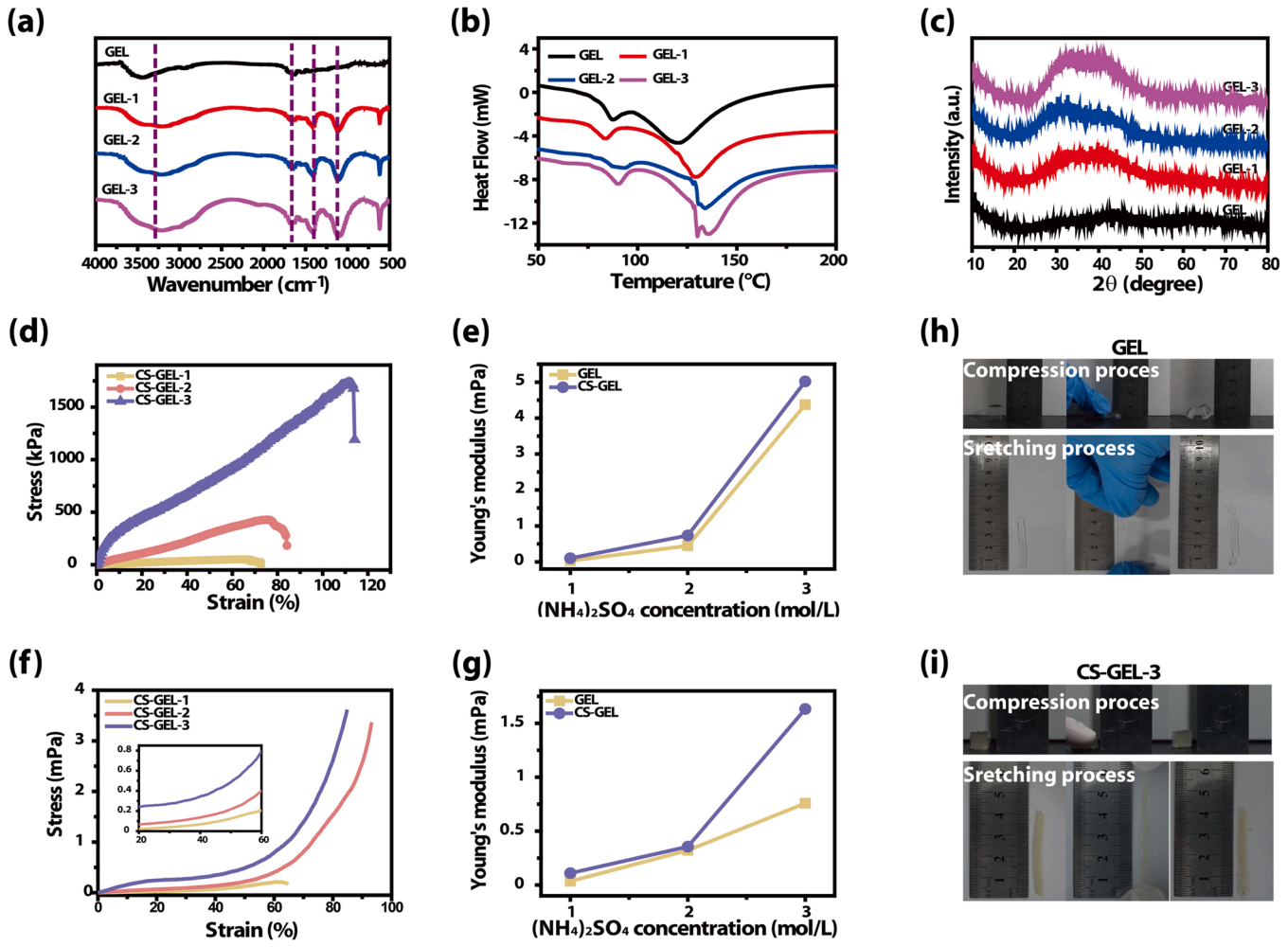

Fig. 3. (a-c) Physical properties of original gelatin before and after gelatin was soaked in the $(NH_4)_2SO_4$ solution with different concentrations (1 mol/L, 2 mol/L, 3 mol/L): (a) FTIR spectra, (b) DSC curves, (c) XRD characterization. (d-g) Mechanical properties of gelatin hydrogel and composite actuator before and after gelatin was soaked in the $(NH_4)_2SO_4$ solution with different concentrations (1 mol/L, 2 mol/L, 3 mol/L). Pictures of (h) compression process and (i) stretching process of gelatin hydrogel and composite actuator.

3 mol/L) for 8 h, and the FTIR results show that the O-H tensile vibration at 3415 cm^{-1}, the -CH_3 symmetric deformation and C-H bending one at 1395 cm^{-1} for gelatin hydrogel increase with the concentration increase of $(NH_4)_2SO_4$ from 1 mol/L to 3 mol/L, indicating a strengthened hydrogen bond interaction between gelatin chains and the improved folding and binding of gelatine molecular chain (Fig. 3a) [33]. At the same time, the strength of the amide I band at 1622 cm^{-1} increases, indicating that the chain bundle and triple helix structure of the hydrogel are strengthened. The signal increase related to sulfate at 1100 cm^{-1} shows that the effect of $(NH_4)_2SO_4$ on the hydrogel structure is more obvious at higher concentrations of $(NH_4)_2SO_4$. In other words, after the pre-formed gelatin hydrogel is soaked in $(NH_4)_2SO_4$ solution, the aggregation of gelatin molecular chain occurs, and the degree of molecular chain aggregation increases with the increase of $(NH_4)_2SO_4$ solution concentration (Fig. 3a) [33]. Moverover, the greater the ionic solubility, the more obvious the salting out effect of gelatin, and the greater the volume shrinkage of gelatin hydrogel. As show in Fig. S7, the composite actuator prepared at − 90 ℃ directional freezing temperature demonstrates the maximum bending angle (730°) and driving speed (5.6°/s) after soaking in 3 mol/L $(NH_4)_2SO_4$ solution (Movie S1). When the composite actuator is placed in the deionized water, the pressure inside the actuator with rich ions is much higher than that of the actuator outside, and the ions are therefore released from the actuator and the actuator recovers with a slowdown speed due to the decreased osmotic pressure. Once the osmotic pressure reaches equilibrium, the recovery of the actuator stops. When we stick a pearl (0.68 g in mass) on the bottom end of the actuator (0.21 g in mass) and put the actuator into the solvent (Fig. S8), the composite actuator can lift the pearl easily, indicating satisfactory driving force and good mechanical properties of the actuator.

The salting-out effect of gelatin also assists the mechanical properties of composite actuator. The molecular chains of gelatine are bound to each other and are strengthened after salting out, which means a greater crystallinity and an improved mechanical properties of gelatin hydrogel. After soaking in different concentrations of ammonium sulfate solution (1 mol/L, 2 mol/L, 3 mol/L) and deionized water, the gelatin hydrogels were tested by differential scanning calorimeter (DSC). The peak value of the heat flow curve measured by DSC can be considered as the result of partial melting of gelatin hydrogel crystals. The Melting enthalpy of crystallinity (Hcrystalline) per unit mass of dried gelatin can be calculated by the integral of endothermic transition. Therefore, the mass of crystallinity can be given as [39].

$$m_{crystalline} = m \times H_{crystalline}/H^{0}_{crystalline} \quad (1)$$

Here $H^{0}_{crystalline}$ is the enthalpy of melting at a 100% crystallinity of gelatin, and m is the mass of the sample. Therefore, the crystallinity X_{dry} of the dried gelatin can be calculated as [39].

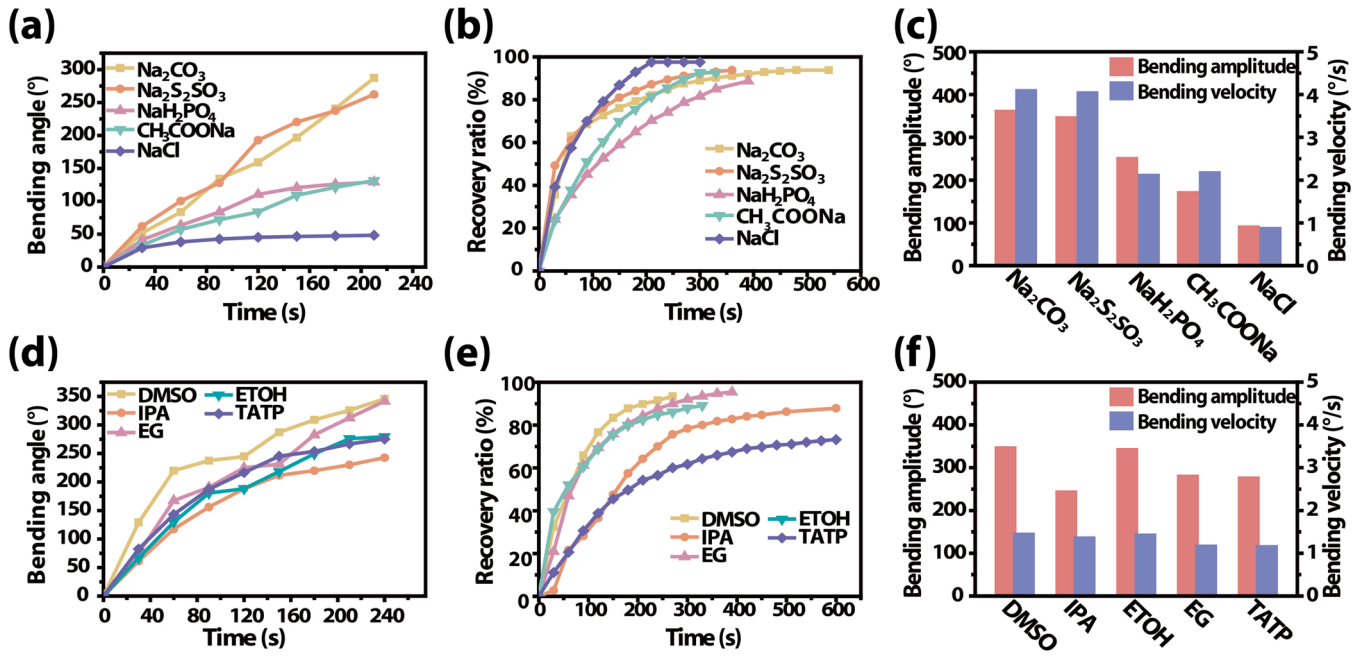

Fig. 4. (a-c) Effects of different ionic solutions on (a) bending, (b) recovery ratio, (c) bending amplitude and initial bending velocity of composite actuator in deformation process. (d-h) Effects of different organic solvents on (d) bending, (e) recovery ratio, (h) bending amplitude and initial bending velocity of composite actuator in deformation process.

$$X_{dry} = m_{crystalline} / m \quad (2)$$

According to the measured water content F_{water}, the crystallinity in the swellen state can be calculated as [39].

$$X_{swellen} = X_{dry} \times (1 - F_{water}) \quad (3)$$

In summary, as long as the peak value of DSC heat flow curve is larger, the crystallinity of gelatin hydrogel is larger, indicating that the molecular chain of gelatin hydrogel is more concentrated. As shown in the heat flow curve of DSC in Fig. 3b, two peaks appear at about 85 ℃ and 125 ℃, and the peak at 125 ℃ becomes larger with the increase of ionic solubility.The 85 ℃ peak is due to the evaporation of water in the gelatin hydrogel. The peak at 125 ℃ is the result of partial melting of gelatin hydrogel crystals. The larger the peak, the larger the enthalpy of melting. As the ionic solubility increases, the F_{water} of gelatin decreases and the $H_{crystallization}$ of gelatin increases, therefore the $X_{swellen}$ of gelatin increases. The XRD data also verify this point. The XRD image of gelatin hydrogel after soaking in deionized water shows a gentle curve,

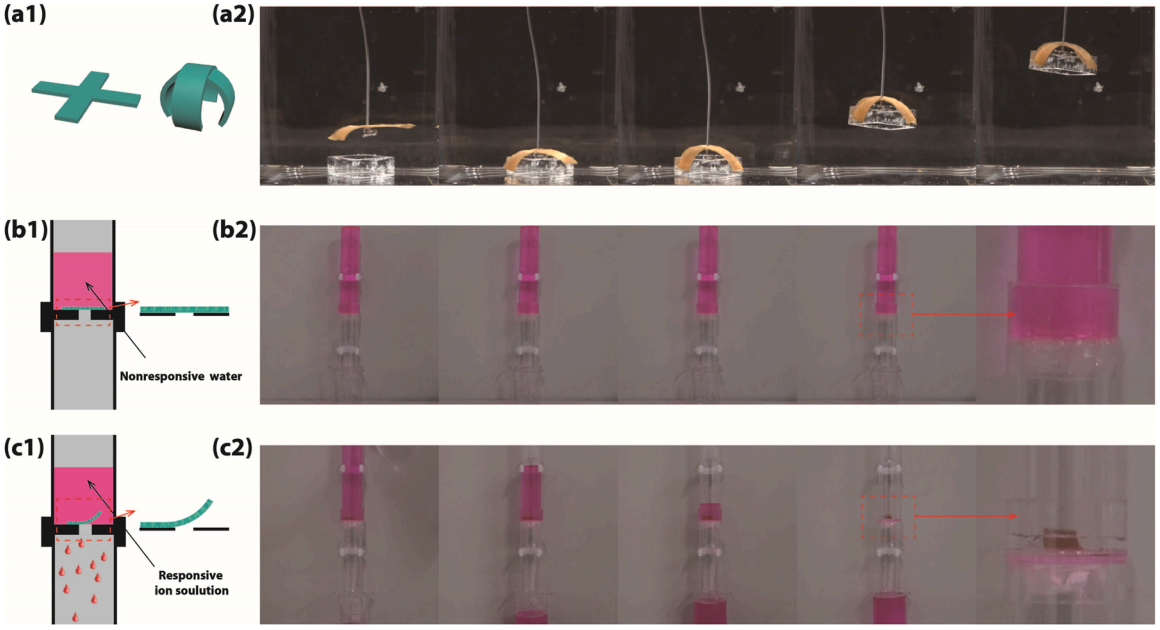

Fig. 5. Application of composite actuator as (a1-a2) a gripper to grab the target object, and (b-c) an intelligent microfluidic valve to control the flowing of different solutions including (b1-b2) deionized water and (c1-c2) $(NH_4)_2SO_4$ solution.

indicating that there is no crystalline part of gelatin hydrogel at this time. However, for XRD images of gelatin hydrogel soaked in ammonium sulfate solution, it can be seen that a mantou peak appears in the 2θ rang from 20° to 40°, whose intensity increases with the increase of ion concentration of $(NH_4)_2SO_4$ solution (Fig. 3c), hinting the enhancement of crystallinity of gelatin hydrogel. The increased crystallinity of gelatin hydrogel further contributes to the mechanical property improvement. As shown in Fig. S9, after immersion in the $(NH_4)_2SO_4$ solution (3 mol/L), the maximum tensile stress and compression stress of gelatin hydrogel (GEL-3) rise up to 1.6 MPa and 5.1 MPa, respectively, presenting several times growth in deformation quantity when compared to unsoaked gelatin hydrogel. The aerogel skeleton also plays an important role in improving the mechanical properties of composite actuator. Compared with gelatine gel, the maximum tensile stress of the composite actuator (CS-GEL-3) is 1.9 MPa and the maximum compressive stress is 3.5 MPa (Fig. 3d and 3f). Though there is a certain degree of reduction in the maximum tensile and compressive strains of the composite actuator after immersion in the ionic solution with high concentration, the improvement of mechanical properties is still obvious when compared to gelatin hydrogel under the same treatment conditions (Fig. 3e and 3g). The addition of aerogel skeleton restricts the tension and compression deformation of gelatin hydrogel to a certain extent, but increases the stiffness of composite, making it not easy to grind and break (Fig. 3h and i).

3.3. Multiple-solvent responsiveness and intelligent valve application of composite actuator

The multi-solvent responsiveness of composite actuator is further investigated when considering the Hofmeister effect and corresponding ionic sequence ($CO_3^{2-}>SO_4^{2-}>S_2O_3^{2-}>H_2PO^{4-}>F^->CH_3COO^->Cl^->Br^->NO_3^-$>$I^-$>$ClO_4^-$>$SCN^-$). Here we selected five ionic solutions for in-depth study, namely Na_2CO_3, $Na_2S_2O_3$, NaH_2PO_4, CH_3COONa and NaCl solution. The driving speed and maximum bending angle of composite actuator in different ionic solutions are consistent with the law of Hofmeister sequence (Fig. 4a-c, Fig. S10 and Movie S2). Additionally, ethanol, acetone and some organic solvents containing a large number of hydroxyl and carbonyl groups can also make protein salting out and denaturatio by forming hydrogen bonds with proteins, reducing solvent dielectric constant, and increasing the attraction to opposite electric charge. As shown in Fig. 4d-f and Fig. S11, the composite actuator has the responsiveness in dimethyl sulphoxide (DMSO), isopropano (IPA), glycol (EG), acetone (TATP) and ethyl alcohol (ETOH) solvents, and finishes corresponding bending and recover deformation (Movie S3). Therefore, the composite actuator has a good adaptability in a changing environment.

Supplementary material related to this article can be found online at doi:10.1016/j.snb.2023.133932.

Supplementary material related to this article can be found online at doi:10.1016/j.snb.2023.133932.

Based on the good mechanical properties and multiple solution responsiveness of composite actuator, it can be intentionally designed for different geometric dimensions to achieve special deformation. For example, a four-arm gripper with a thickness of 1 mm is manufactured by a cross-shaped mold, which can grab the target object in the ionic solution (Fig. 5a1-a2). An intelligent valve (2 cm × 2 cm×1 mm in length×width×thickness) is also constructed and fixed at one end into the middle of baffle pipe with a hole (0.5 cm in diameter). When the deionized water is poured into the pipe, the deionized water can't pass through the hole due to tightly closed hole by the valve (composite actuator) under liquid pressure (Fig. 5b1-b2). When a salt solution, for example $(NH_4)_2SO_4$ solution, is poured into the pipe, the movable end of the valve (with macropores face up) bends upward towards the salt solution, exposing holes in the baffle to allow salt solution to flow down (Fig. 5c1-c2). By changing the concentration of salt solution, for example $(NH_4)_2SO_4$ solution (1 mol/L, 2 mol/L, 3 mol/L), the flow rate of salt solution is very easy to control due to the concentration dependent actuation behavior of composite actuator (Fig. S12, Movie S4). The valve can not only let specific solutions pass through, but also identify the types of solutions according to the flow rates of different solutions, providing a promising application of composite actuator in intelligent valves.

Supplementary material related to this article can be found online at doi:10.1016/j.snb.2023.133932.

4. Conclusion

Inspired by the combination of human bones and muscles, we report a aerogel/hydrogel composite actuator with directional structured chitosan aerogel as the skeleton and solvent-sensitive gelatin hydrogel as muscle in the actuator framework. By optimizing the pore structures of chitosan aerogel and mechanical properties of gelatin hydrogel, the composite actuator exhibits multimodal deformation in a variety of ionic and organic solvents, and has good recovery in deionized water. At the same time, the mechanical properties of the composite actuator are amazing with the maximum tensile stress and compressive stress up to 1.9 MPa and 3.5 MPa, respectively. The well-designed composite actuator can serve as a mechanical grip and an intelligent microfluidic valve to grab the target object, and to control the flowing of different solutions with different flow rates. The proposed hydrogel-based composite actuator can provide design inspiration for soft robots, smart actuators, artificial muscles, and intelligent human-machine interface technology.

CRediT authorship contribution statement

Zhongwen Kuang: Writing – original draft, Data curation, Validation. **Weizhong Xu:** Writing – original draft, Data curation, Validation. **Jiaxin Li:** Data curation, Validation. **Zhuanzhuan Fan:** Data curation, Validation. **Ruofei Wang:** Data curation, Validation. **Shanpeng Ji:** Investigation. **Chengnan Qian:** Formal analysis, Validation. **Lin Cheng:** Investigation. **Huaping Wu:** Investigation. **Aiping Liu:** Writing – review & editing, Project administration.

Declaration of Competing Interest

The authors declare that they have no known competing financial interests or personal relationships that could have appeared to influence the work reported in this paper.

Data Availability

Data will be made available on request.

Acknowledgements

This work was supported by the National Natural Science Foundation of China (Nos. 12272351, 11672269 and 11972323), the Youth Top-notch Talent Project of Zhejiang Ten Thousand Plan of China (No. ZJWR0308010), and the Zhejiang Provincial Natural Science Foundation of China (Nos. LR20A020002 and LR19E020004).

Appendix A. Supporting information

Supplementary data associated with this article can be found in the online version at doi:10.1016/j.snb.2023.133932.

References

[1] X. Yao, J. Liu, C. Yang, X. Yang, J. Wei, Y. Xia, X.Y. Gong, Z. Suo, Hydrogel paint, Adv. Mater. 31 (2019) 1903062.
[2] H. Yuk, T. Zhang, T. Lin, G.A. Parada, X.H. Zhao, Tough bonding of hydrogels to diverse non-porous surfaces, Nat. Mater. 15 (2016) 190–196.

[3] Y.X. Liu, J. Liu, S.C. Chen, T. Lei, Y.G. Kim, S.M. Niu, H.L. Wang, X. Wang, A. M. Foudeh, J.B.H. Tok, Z.N. Bao, Soft and elastic hydrogel-based microelectronics for localized low-voltage neuromodulation, Nat. Biomed. Eng. 3 (2019) 58–68.
[4] Y. Huang, M. Zhong, F. Shi, X.Y. Liu, Z.J. Tang, Y.K. Wang, Y. Huang, H.Q. Hou, X. M. Xie, C.Y. Zhi, A polyacrylamide hydrogel electrolyte enabled intrinsically 1000% stretchable and 50% compressible supercapacitor, Angew. Chem. Int. Ed. 56 (2017) 9141.
[5] K.Y. Lee, D.J. Mooney, Hydrogels for tissue engineering, Chem. Rev. 101 (2001) 1869–1880.
[6] Y. Tan, D. Wang, H. Xu, Y. Yang, X.L. Wang, F. Tian, P. Xu, W. An, X.M. Zhao, S. Xu, Rapid recovery hydrogel actuators in air with bionic large-ranged gradient structure, Acs Appl. Mater. Inter 10 (2018) 40125–40131.
[7] M. Bassil, M. Ibrahim, M. El Tahchi, Artificial myscular microfibers: hydrogel with high speed tunable electroactivity, Soft Matter 7 (2011) 4833–4838.
[8] M. Wehner, R.L. Truby, D.J. Fitzgerald, B. Mosadegh, G.M. Whitesides, J.A. Lewis, R.J. Wood, An integrated design and fabrication strategy for entirely softe, autonomous robots, Nature 536 (2016) 451–455.
[9] H. Yuk, S. Lin, C. Ma, M. Takaffoli, N.X. Fang, X. Zhao, Hydraulic hydrogel actuators and robots optically and sonically camouflaged in water, Nat. Commun. 8 (2017) 14230.
[10] C. Yao, Z. Liu, C. Yang, W. Wang, X.J. Ju, R. Xie, L.-Y. Chu, Poly(N-isopropylacrylamide)-clay nanocomposite hydrogels with responsive bending property as temperature-controlled manipulators, Adv. Funct. Mater. 25 (2015) 2980–2991.
[11] K. Liu, Y. Zhang, H. Cao, H. Liu, Y. Geng, W. Yuan, J. Zhou, Z.L. Wu, G. Shan, Y. Bao, Q. Zhao, T. Xie, P. Pan, Programmable reversible shape transformation of hydrogels based on transient structural anisotropy, Adv. Mater. 32 (2020) 2001693.
[12] C. Li, A. Iscen, H. Sai, K. Sato, N.A. Sather, S.M. Chin, Z. Álvarez, L.C. Palmer, G. C. Schatz, S.I. Stupp, Supramolecular-covalent hybrid polymers for light-activated mechanical actuation, Nat. Mater. 19 (2020) 900–909.
[13] R. Luo, J. Wu, N.-D. Dinh, C.-H. Chen, Gradient porous elastic hydrogels with shape-memory property and anisotropic responses for programmable locomotion, Adv. Funct. Mater. 25 (2015) 7272–7279.
[14] E.Z. Zhang, T. Wang, W. Hong, W.X. Sun, X.X. Liu, Z. Tong, Infrared-driving actuation based on bilayer graphene oxide-poly(N-isopropylacrylamide) nanocomposite hydrogels, J. Mater. Chem. A. 2 (2014) 15633–15639.
[15] Y. Jian, B. Wu, X. Le, Y. Liang, Y. Zhang, D. Zhang, L. Zhang, W. Lu, J. Zhang, T. Chen, Antifreezing and stretchable organohydrogels as soft actuators, Research 2019 (2019) 2384347.
[16] Z. Li, P. Liu, X. Ji, J. Gong, Y. Hu, W. Wu, X. Wang, H.-Q. Peng, R.T.K. Kwok, J.W. Y. Lam, J. Lu, B.Z. Tang, Bioinspired simultaneous changes in fluorescence color, brightness, and shape of hydrogels enabled by AIEgens, Adv. Mater. 32 (2020) 1906493.
[17] S.Y. Zheng, Y. Shen, F. Zhu, J. Yin, J. Qian, J. Fu, Z.L. Wu, Q. Zheng, Programmed deformations of 3D-printed tough physical hydrogels with high response speed and large output force, Adv. Funct. Mater. 28 (2018) 1803366.
[18] X. Du, H. Cui, Q. Zhao, J. Wang, H. Chen, Y. Wang, Inside-out 3D reversible ion-triggered shape-morphing hydrogels, Research 2019 (2019) 6398296.
[19] X. Peng, T. Liu, Q. Zhang, C. Shang, Q.-W. Bai, H. Wang, Surface patterning of hydrogels for programmable and complex shape deformations by ion inkjet printing, Adv. Funct. Mater. 27 (2017) 1701962.
[20] H. Qin, T. Zhang, N. Li, H.P. Cong, S.-H. Yu, Anisotropic and self-healing hydrogels with multi-responsive actuating capability, Nat. Commun. 10 (2019) 2202.
[21] H. Jiang, L. Fan, S. Yan, F. Li, H. Li, J. Tang, Tough and electro-responsive hydrogel actuators with bidirectional bending behavior, Nanoscale 11 (2019) 2231–2237.
[22] A. López-Díaz, A. Martín-Pacheco, A.M. Rodríguez, M.A. Herrero, A.S. Vázquez, E. Vázquez, Concentration gradient-based soft robotics: hydrogels out of water, Adv. Funct. Mater. 30 (2020) 2004417.
[23] R. Tognato, A.R. Armiento, V. Bonfrate, R. Levato, J. Malda, M. Alini, D. Eglin, G. Giancane, T. Serra, A. Stimuli-Resoinsive, Nanocomposite for 3D anisotropic cell-guidance and magnetic soft robotics, Adv. Funct. Mater. 29 (2019) 1804647.
[24] D. Rus, M.T. Tolley, Design, fabrication and control of soft robots, Nature 521 (2015) 467–475.
[25] X. Le, W. Lu, J. Zhang, T. Chen, Recent progress in biomimetic anisotropic hydrogel actuators, Adv. Sci. 6 (2019) 1801584.
[26] S. Li, H. Bai, R.F. Shepherd, H. Zhao, Bio-inspired design and additive manufacturing of soft materials, machines, robot, and haptic interfaces, Angew. Chem., Int. Ed. 58 (2019) 11182–11204.
[27] P.L. Dong, W.Z. Xu, Z.W. Kuang, Y.X. Yao, Z.Q. Zhang, D.Y. Guo, H.P. Wu, T. Y. Zhao, A.P. Liu, Liquid stratification and diffusion-induced anisotropic hydrogel actuators with excellent thermosensitivity and programmable functionality, Adv. Intell. Syst. 3 (2021) 2100030.
[28] Y. Wang, Y.J. Wang, Anisotropic diffusion filtering method with weighted directional structure tensor, Biomed. Signal Proces. 53 (2019), 101590.
[29] S.K. Seidlits, Z.Z. Khaing, R.R. Petersen, J.D. Nickels, J.E. Vanscoy, J.B. Shear, C. E. Schmidt, The effects of hyaluronic acid hydrogels with tunable mechanical properties on neural progenitor cell differentiation, Biomaterials 31 (2010) 3930–3940.
[30] L. Han, X. Lu, K. Liu, K.F. Wang, L.M. Fang, L.T. Weng, H.P. Zhang, Y.H. Tang, F. Z. Ren, C.C. Zhao, G.X. Sun, R. Liang, Z.J. Li, Mussel-inspired adhesive and tough hydrogel based on nanoclay confined dopamine polymerization, ACS nano 11 (2017) 2561–2574.
[31] S. Lin, J. Liu, X. Liu, X.H. Zhao, Muscle-like fatigue-resistant hydrogels by mechanical training, PNAS Latest Artic. 116 (2019) 10244–10249.
[32] X. Zhao, Multi-scale multi-mechanism design of tough hydrogels: building dissipation into stretchy networks, Soft Matter 10 (2014) 672–687.
[33] Q. He, Y. Huang, S. Wang, Hofmeister effect-assisted one step fabrication of ductile and strong gelatin hydrogels, Adv. Funct. Mater. 28 (2018) 1705069.
[34] W.Z. Xu, Y. Xing, J. Liu, H.P. Wu, Y. Cui, D.W. Li, D.Y. Guo, C.R. Li, A.P. Liu, H. Bai, Efficient water transport and solar steam generation via radially, hierarchically structured aerogels, ACS nano 13 (2019) 7930–7938.
[35] H. Bai, Y. Chen, B. Delattre, A.P. Tomsia, R.O. Ritchie, Bioinspired large-scale aligned porous materials assembled with dual temperature gradients, Sci. Adv. 1 (2015) 1500849.
[36] H.L. Gao, Y. Lu, L.B. Mao, D. An, L. Xu, J.T. Gu, F. Long, S.H. Yu, A shape-memory scaffold for macroscale assembly of functional nanoscale building blocks, Mater. Horiz. 1 (2014) 69–73.
[37] H. Muta, M. Miwa, M. Satoh, Ion-specific swelling of hydrophilic polymer gels, Polymer 42 (2001) 6313–6316.
[38] Y. Zhang, S. Furyk, D.E. Bergbreiter, P.S. Cremer, Specific ion effects on the water solubility of macromolecules: PNIPAM and the Hofmeister series, J. Am. Chem. Soc. 127 (2005) 14505–14510.
[39] M.T. Hua, S.W. Wu, Y.F. Ma, Y.S. Zhao, Z.L. Chen, I. Frenkel, J. Strzalka, H. Zhou, X.Y. Zhu, X.M. He, Strong tough hydrogels via the synergy of freeze-casting and salting out, Nature 590 (2021) 594–599.

Zhongwen Kuang received his Master Degree in Materials Engineering from Zhejiang Sci-Tech University in 2022. His research interest is developing novel functional materials for flexible hydrogel actuator and sensors.

Weizhong Xu received his Doctoral Degree in Mechanical Engineering from Zhejiang Sci-Tech University in 2022. His research interest is developing novel functional materials for flexible hydrogel actuator and sensors.

Jiaxin Li received her Bachelor Degree in Materials Physics Engineering from Nanjing University of Information Science & Technology in 2020. She is currently pursuing a master's degree in Zhejiang Sci-Tech University. His research interest is developing novel functional materials for flexible hydrogel actuator and sensors.

Zhuanzhuan Fan received her Bachelor Degree in Applied physics from Zhejiang Sci-Tech University in 2020. She is currently pursuing a master's degree in Zhejiang Sci-Tech University. Her research interest is developing novel functional materials for flexible hydrogel actuators and sensors.

Ruofei Wang received his Bachelor Degree in Applied physics from Zhejiang Sci-tech University in 2020. He is currently pursuing a master's degree in Zhejiang Sci-Tech University. His research interest is developing novel functional materials for flexible hydrogel actuator and sensors.

Shanpeng Ji received his Bachelor Degree in Applied physics from Zhejiang Sci-tech University in 2020. He is currently pursuing a master's degree in Zhejiang Sci-Tech University. His research interest is developing novel functional materials for wearable physical sensors.

Chengnan Qian received his Bachelor Degree in New Energy Materials and Devices from Zhejiang Sci-Tech University in 2022. He is currently pursuing a master's degree in Zhejiang Sci-Tech University. His research interest is developing novel functional materials for flexible hydrogel actuators and sensors.

Lin Cheng received her Bachelor degree in Science from Zhejiang Sci-Tech University in 2013 and received her Master's degree from Henan University in 2017. She is currently pursuing a Ph.D. degree from the School of Materials Science and Engineering, Zhejiang Sci-Tech University. Her research interests include flexible sensor and smart materials/structures.

Prof. Huaping Wu received his Ph. D degree in Engineering Mechanics from the Harbin Institute of Technology in 2009 and a Bachelor's degree from the Harbin Institute of Technology in 2002. He worked as a visiting scholar at the Kyoto University in 2014 and a postdoctoral research fellow at the City University of Hong Kong in 2012. He is currently a Professor in the School of Mechanical Engineering at Zhejiang University of Technology. His research mainly focuses on the mechanics of smart materials/structures, bionic machinery and bionic manufacturing, and flexible electronics devices.

Prof. Aiping Liu received her Ph.D. degree in Material Science from the Harbin Institute of Technology in 2008. She worked as a postdoctoral research fellow at the Nanyang Technological University from 2009 to 2011 and a visiting scholar at the University of Texas at Austin from 2019 to 2020. She is currently a Professor in the Department of Physics at Zhejiang Sci-Tech University. Her research mainly focuses on the functional inorganic/organic material, with special emphasis on developing novel materials including graphene with sensing and actuation characteristic for wearable physical/chemical sensors and intelligent actuators.